Pergamon

PII: S0301-9322(96)00068-7

Int. J. Multiphase Flow Vol. 23, No. 3, pp. 545–560, 1997

Printed in Great Britain
0301-9322/97 $17.00 + 0.00

TWO-PHASE MAGNETOHYDRODYNAMIC FLOW AND HEAT TRANSFER IN AN INCLINED CHANNEL

M. S. MALASHETTY and J. C. UMAVATHI
Department of Mathematics, Gulbarga University, Gulbarga 585 106, India

(Received 10 January 1996; in revised form 19 September 1996)

Abstract—Two-phase MHD flow and heat transfer in an inclined channel is investigated in which one phase being electrically conducting. The transport properties of both fluids are assumed constant. The resulting governing equations are coupled and nonlinear. An approximate solution is obtained using perturbation method. The results are presented for various values of the ratios of viscosities, thermal conductivities, heights of the fluid, Hartmann number, Grashof number and angle of inclination. It is found that the velocity and temperature can be increased or decreased with suitable values of the ratios of viscosities, thermal conductivities, the heights and the angle of inclination. © 1997 Elsevier Science Ltd. All rights reserved.

Key Words: MHD, two-phase, inclined, heat transfer

1. INTRODUCTION

In the petroleum industry, as well as in other engineering fields, stratified two-phase flow often occurs. There has been some experimental and analytical studies on hydrodynamic aspects of two-phase flow reported in the recent literature. The interest in these types of problems stems from the possibility of reducing the power required to pump oil in a pipeline by suitable addition of water. Packham and Shail (1971) analyzed stratified laminar flow of two immiscible liquids in a horizontal pipe. Hartmann flow of a conducting fluid in a channel with a layer of nonconducting fluid between upper channel wall and the conducting fluid has been studied by Shail (1973). He found that an increase of the order 30% can be achieved in the flow rate for suitable ratios of depths and viscosities of the two fluids.

The advent of technology in the field of MHD power generators and MHD devices, nuclear engineering and thermonuclear power has created a great practical need for understanding the dynamics of conducting fluids. The use of liquid metals as heat transfer agents and as working fluids in MHD power generators has created a growing interest in the study of liquid metal flows and nature of interaction with magnetic field. The interaction between the conducting fluid and magnetic field radically modifies the flow and heat transfer characteristics.

The outlook for a direct coal-fired MHD power generator as potentially significant source of energy seems promising in view of its efficiency, its effect on environment and the availability of needed natural resources. The first investigation associated with two-phase liquid metal magnetofluidmechanics generator project at the Argonne National Laboratory were by Thome (1964). Postlethwaite and Sluyter (1978) have reviewed extensively the heat transfer problems associated with MHD generators. Lohrasbi and Sahai (1988) studied two-phase MHD flow and heat transfer in a parallel plate channel, with the fluid in one phase being conducting. Recently, Malashetty and Leela (1991, 1992) studied two-phase flow and heat transfer characteristics in a horizontal channel with the fluids in both phases being electrically conducting. These studies are useful in understanding the effect of the presence of a slag layer on heat transfer characteristics of a coal-fired MHD generator.

The inclined geometry has received considerable attention in the heat transfer literature, attention undoubtedly stimulated by the growing interest in solar collector technology. The basic research in this area has been reviewed by Raithby and Hollands (1976) and Catton (1978). However, the study of flow and heat transfer in two-phase inclined channel has not received any attention even though the problem is of practical importance in many areas of technology.

Our study is motivated by the work of Lohrasbi and Sahai (1988) who investigated the effect of slag layer on the heat transfer characteristics of MHD generator channels. In the present problem, two-phase MHD flow and heat transfer in an inclined channel is studied.

2. MATHEMATICAL FORMULATION

The geometry under consideration illustrated in figure 1, consists of two infinite inclined parallel plates maintained at different constant temperatures, extending in the z and x-directions, making an angle ϕ with the horizontal. The region $0 \leqslant y \leqslant h_1$ is occupied by an electrically nonconducting fluid of density ρ_1, viscosity μ_1, thermal conductivity K_1 and the region $-h_2 \leqslant y \leqslant 0$ is occupied by a different (immiscible) electrically conducting fluid of density ρ_2, viscosity μ_2, electrical conductivity σ and thermal conductivity K_2. The transport properties of both fluids are assumed constant. A constant magnetic field of strength B_0 is applied transverse to the flow field. The flow of both phases is assumed to be driven by a constant pressure gradient $(-\partial p/\partial x)$. We consider the fluids to be incompressible and the flow is steady, laminar and fully developed.

Under these assumptions, the governing equation of motion and energy for Boussinesq fluids are:

For phase I

$$\mu_1 \frac{d^2u_1}{dy^2} + \rho_1 g \beta_1 \sin\phi(T_1 - T_{W2}) = \frac{\partial p}{\partial x} \quad [1]$$

$$\frac{d^2T_1}{dy^2} + \frac{\mu_1}{K_1}\left(\frac{du_1}{dy}\right)^2 = 0. \quad [2]$$

For phase II

$$\mu_2 \frac{d^2u_2}{dy^2} + \rho_2 g \beta_2 \sin\phi(T_2 - T_{W2}) + \sigma B_0^2 u_2 = \frac{\partial p}{\partial x} \quad [3]$$

$$\frac{d^2T_2}{dy^2} + \frac{\mu_2}{K_2}\left(\frac{du_2}{dy}\right)^2 + \frac{\sigma B_0^2 u_2^2}{K_2} = 0, \quad [4]$$

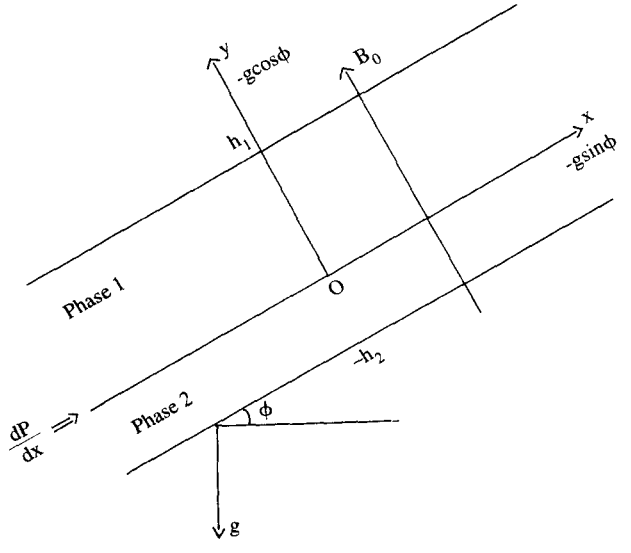

Figure 1. Physical configuration.

where u is the x-component of velocity, T is the temperature, β is the coefficient of thermal expansion, g is the acceleration due to gravity. The suffixes 1 and 2 denote the values for phase I and II, respectively.

The fluid and the thermometric boundary conditions are unchanged by the addition of electromagnetic field. The noslip condition requires that the velocity must vanish at the wall. In addition the fluid velocity, shear stress, temperature and heat flux must be continuous across the interface.

Referring to figure 1, the boundary and interface conditions on velocity are,

$$\begin{gathered} u_1(h_1) = 0 \\ u_1(0) = u_2(0) \\ u_2(-h_2) = 0 \\ \mu_1 \mathrm{d}u_1/\mathrm{d}y = \mu_2 \mathrm{d}u_2/\mathrm{d}y \text{ at } y = 0. \end{gathered} \tag{5}$$

Since the walls are maintained at constant different temperatures T_{w1} and T_{w2} at $y = h_1$ and $y = -h_2$, respectively, the boundary conditions on T_1 and T_2 are given by

$$\begin{gathered} T_1(h_1) = T_{w1} \\ T_1(0) = T_2(0) \\ T_2(-h_2) = T_{w2} \\ K_1 \mathrm{d}T_1/\mathrm{d}y = K_2 \mathrm{d}T_2/\mathrm{d}y \quad \text{at} \quad y = 0. \end{gathered} \tag{6}$$

It is convenient to transform [1]–[4] to a nondimensional form. The following transformations are used:

$$\begin{gathered} u_1^* = u_1/\bar{u}_1, \quad u_2^* = u_2/\bar{u}_1, \quad y_1^* = y_1/h_1 \\ y_2^* = y_2/h_2, \quad \theta = (T - T_{w2})/(T_{w1} - T_{w2}) \\ m = \mu_1/\mu_2, \quad k = K_1/K_2, \quad h = h_2/h_1, \quad n = \rho_2/\rho_1, \\ b = \beta_2/\beta_1, \quad \mathrm{Gr} = g\beta_1 h_1^3 (T_{w1} - T_{w2})/\nu_1^2, \quad \mathrm{M} = B_0 h_2 \sqrt{\sigma/\mu_2}, \\ \mathrm{Pr} = \mu_1 C_p/K_1, \quad P = (h_1^2/\mu_1 \bar{u}_1)(\partial p/\partial x), \quad \mathrm{Re} = \bar{u}_1 h_1/\nu_1, \\ \mathrm{Ec} = \bar{u}_1^2/C_p(T_{w1} - T_{w2}). \end{gathered} \tag{7}$$

Here Gr is the Grashof number, Ec is the Eckert number, Pr is the Prandtl number, Re is the Reynolds number, M is the Hartmann number, P is the nondimensional pressure gradient and $\bar{u}_1$ is the average velocity.

With the above nondimensional quantities, the governing equations [1]–[4] become:

Phase I

$$\frac{\mathrm{d}^2 u_1}{\mathrm{d}y^2} + \frac{\mathrm{Gr}}{\mathrm{Re}} \sin \phi \theta_1 = P \tag{8}$$

$$\frac{\mathrm{d}^2 \theta_1}{\mathrm{d}y^2} + \mathrm{Pr\,Ec} \left(\frac{\mathrm{d}u_1}{\mathrm{d}y} \right)^2 = 0. \tag{9}$$

Phase II

$$\frac{\mathrm{d}^2 u_2}{\mathrm{d}y^2} + \frac{\mathrm{Gr}}{\mathrm{Re}} bmnh^2 \sin \phi \theta_2 - \mathrm{M}^2 u_2 = mh^2 P \tag{10}$$

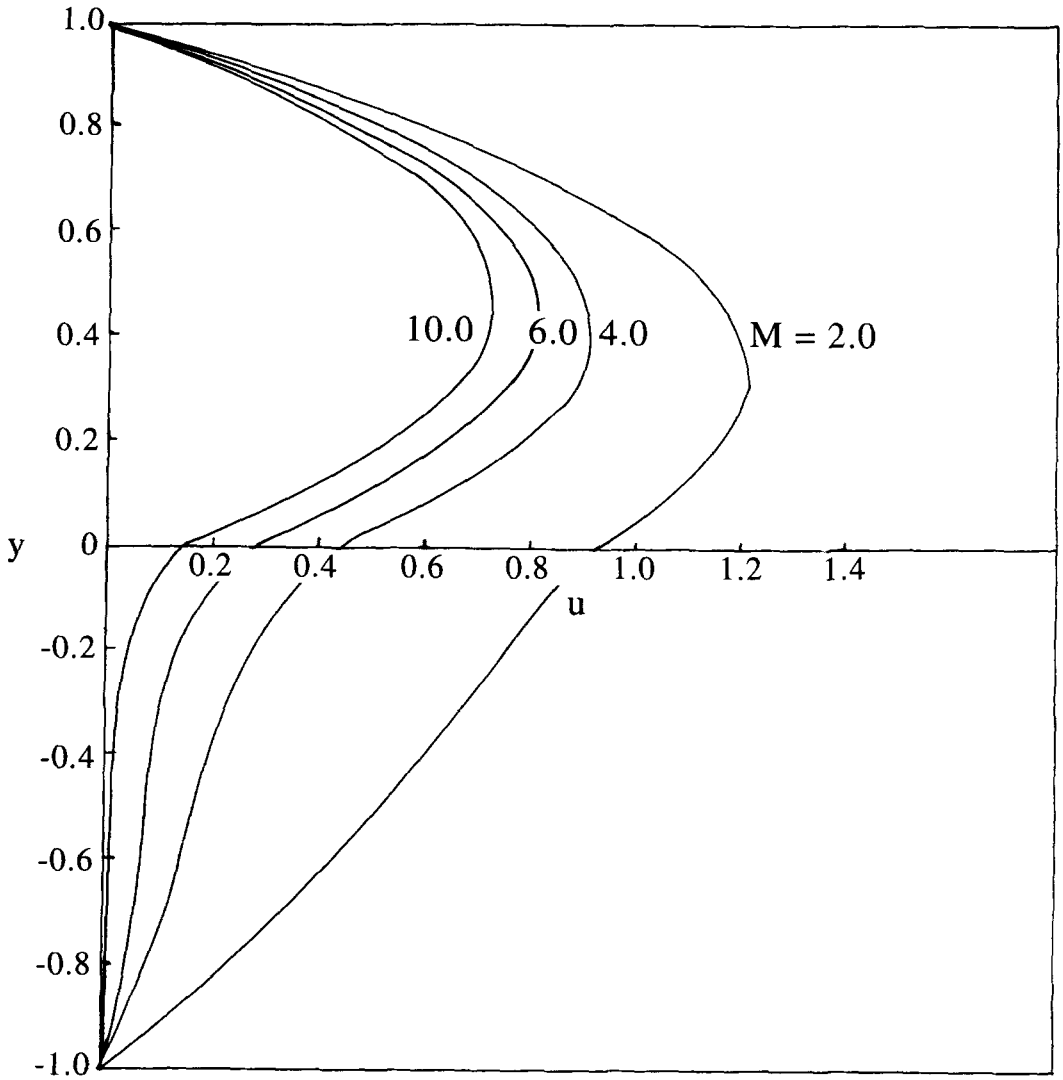

Figure 2. Velocity profiles for different values of M.

$$\frac{d^2\theta_2}{dy^2} + \text{Pr Ec}\left(\frac{k}{m}\right)\left(\frac{du_2}{dy}\right)^2 + \frac{M^2}{m}\text{Pr Ec}\, ku_2^2 = 0. \qquad [11]$$

The asterisks have been dropped with the understanding that all the quantities are now dimensionless.

The nondimensional forms of the velocity, temperature and interface boundary conditions [5] and [6] become:

$$u_1(1) = 0$$

$$u_1(0) = u_2(0) \qquad [12]$$

$$u_2(-1) = 0$$

$$du_1/dy = (1/mh)du_2/dy \quad \text{at} \quad y = 0.$$

$$\theta_1(1) = 1$$

$$\theta_1(0) = \theta_2(0) \qquad [13]$$

$$\theta_2(-1) = 0$$

$$d\theta_1/dy = (1/kh)d\theta_2/dy \text{ at } y = 0.$$

3. SOLUTIONS

The governing equations of momentum [8] and [10], along with the energy equations [9] and [11], are to be solved subject to the boundary and interface conditions [12] and [13] for the velocity and temperature distributions. In this case, the equations are coupled and nonlinear because of the inclusion of the dissipation terms in energy equation. In most of the practical problems the Eckert number is very small and is of order 10^{-5}. Thus the fact that the product Pr Ec $(=\epsilon)$ is very small can be exploited to use the perturbation method. To this end the solutions are assumed in the form:

$$(u_1,\theta_1) = (u_{10},\theta_{10}) + \epsilon(u_{11},\theta_{11}) + \cdots \quad [14]$$

$$(u_2,\theta_2) = (u_{20},\theta_{20}) + \epsilon(u_{21},\theta_{21}) + \cdots \quad [15]$$

where u_{10}, θ_{10}, u_{20}, θ_{20} are solutions for the case ϵ equal to zero. u_{11}, θ_{11}, u_{21}, θ_{21} are perturbed quantities relating to u_{10}, θ_{10}, u_{20}, θ_{20}, respectively. Substituting the above identities in [8]–[11] and

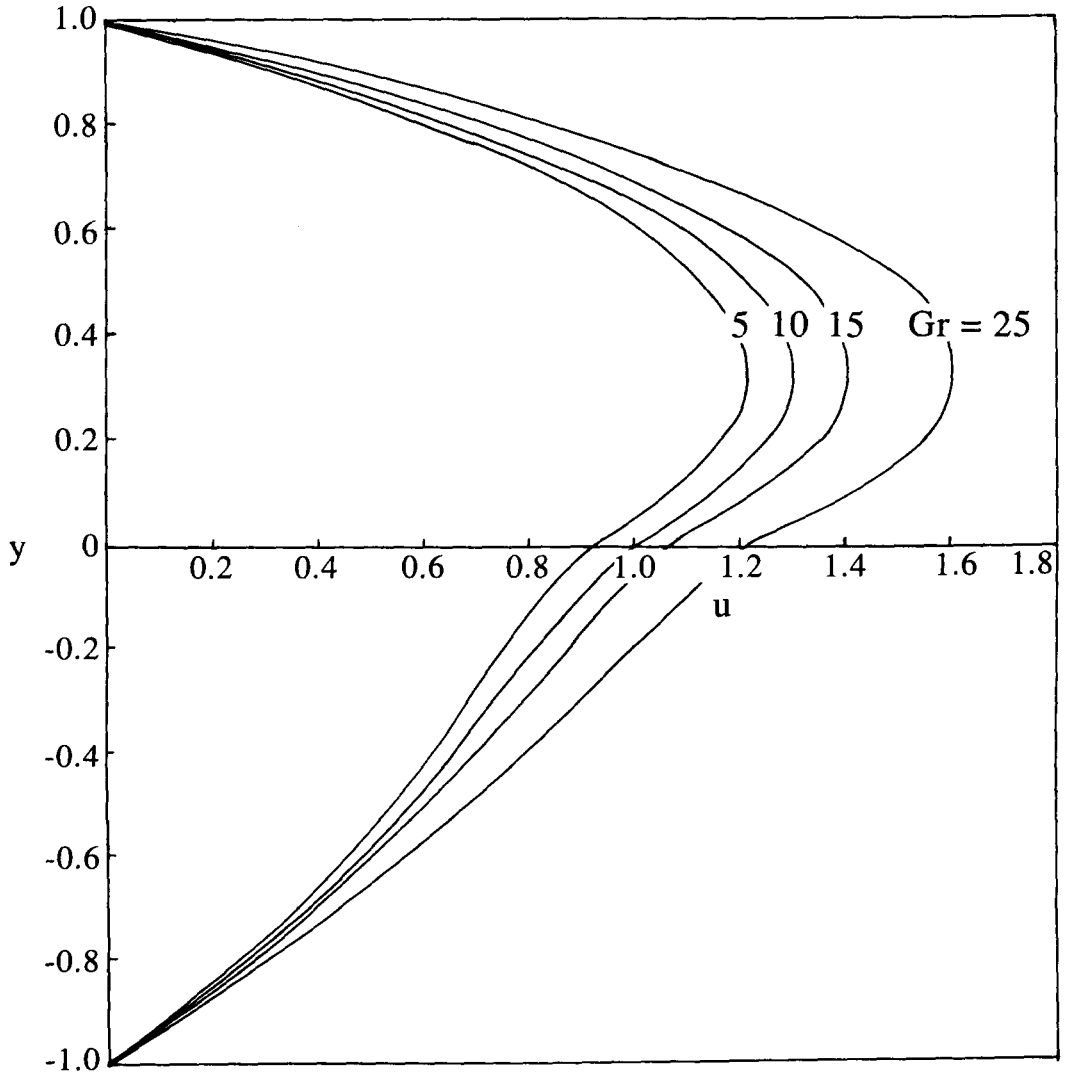

Figure 3. Velocity profiles for different values of Gr.

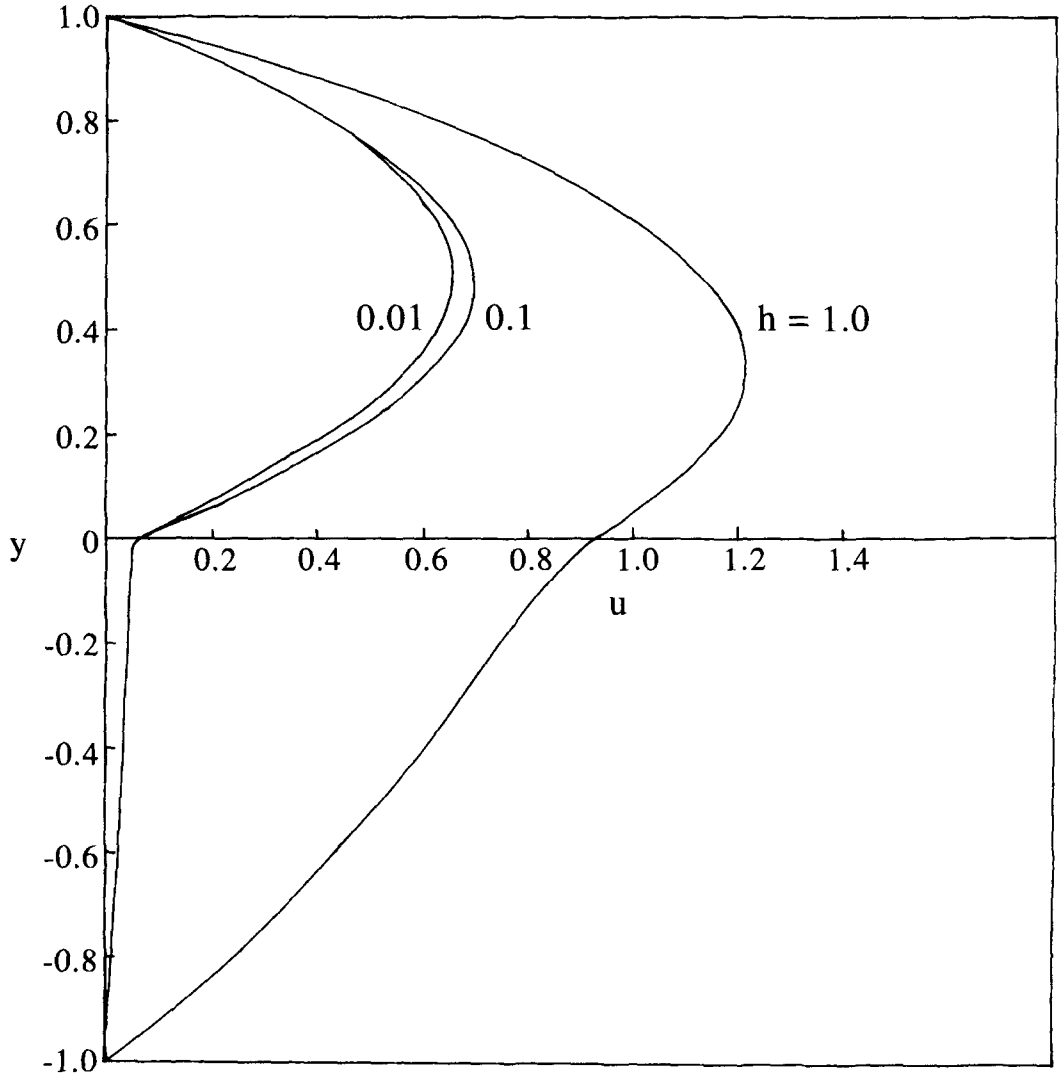

Figure 4. Velocity profiles for different values of h.

equating the coefficients of like powers of ϵ to zero, we get the zeroth and first order equations for phase I and II as follows:

Phase I

Zeroth order equations

$$\frac{d^2u_{10}}{dy^2} + \frac{Gr}{Re}\sin\phi\theta_{10} = P \qquad [16]$$

$$\frac{d^2\theta_{10}}{dy^2} = 0. \qquad [17]$$

First order equations

$$\frac{d^2u_{11}}{dy^2} + \frac{Gr}{Re}\sin\phi\theta_{11} = 0 \qquad [18]$$

$$\frac{d^2\theta_{11}}{dy^2} + \left(\frac{du_{10}}{dy}\right)^2 = 0. \qquad [19]$$

Phase II

Zeroth order equations

$$\frac{d^2u_{20}}{dy^2} + \frac{Gr}{Re}\sin\phi bmnh^2\theta_{20} - M^2u_{20} = mh^2P \qquad [20]$$

$$\frac{d^2\theta_{20}}{dy^2} = 0. \qquad [21]$$

First order equations

$$\frac{d^2u_{21}}{dy^2} + \frac{Gr}{Re}\sin\phi bmnh^2\theta_{21} - M^2u_{21} = 0 \qquad [22]$$

$$\frac{d^2\theta_{21}}{dy^2} + \left(\frac{k}{m}\right)\left(\frac{du_{20}}{dy}\right)^2 + M^2\left(\frac{k}{m}\right)u_{20}^2 = 0. \qquad [23]$$

The corresponding boundary conditions [12] and [13] reduce to:

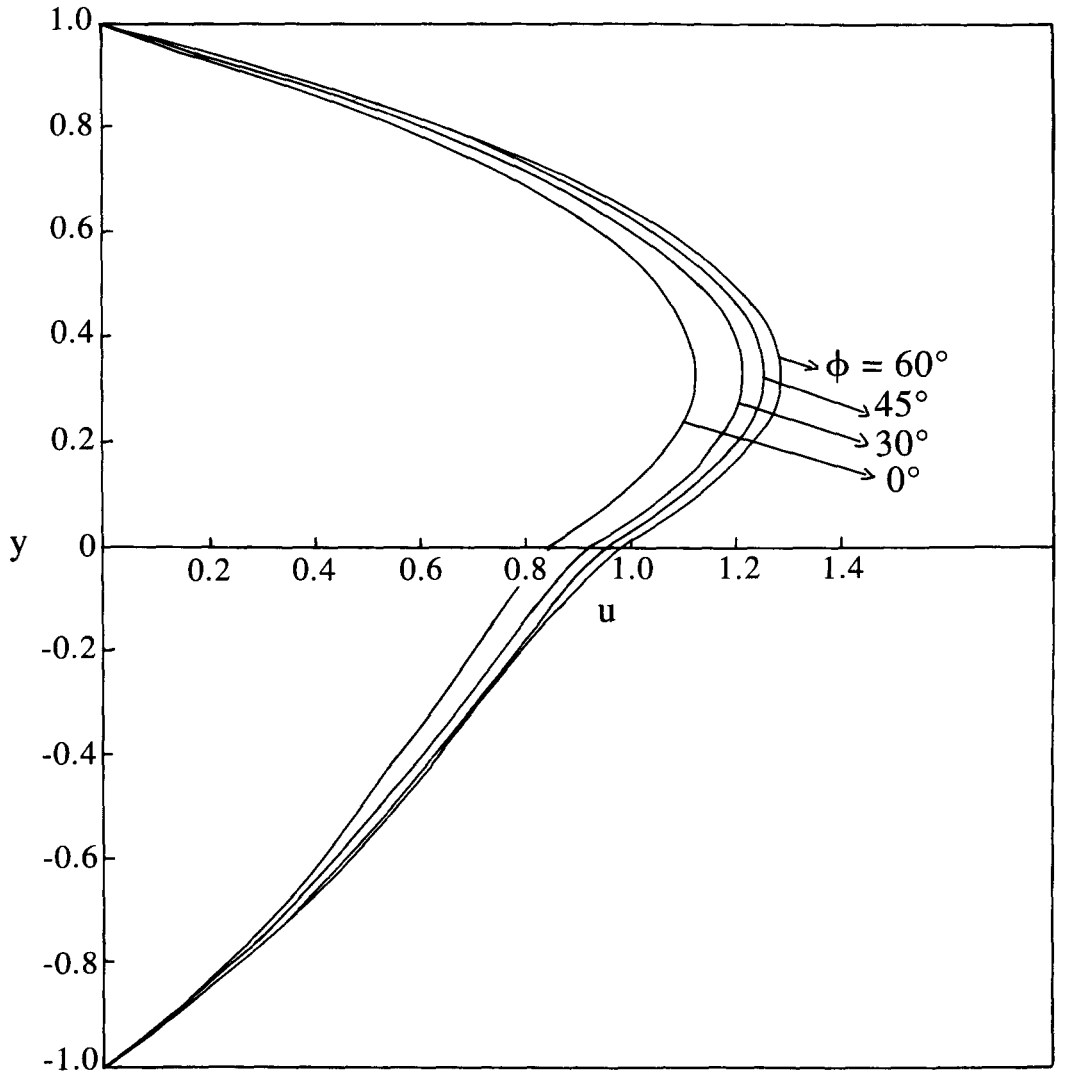

Figure 5. Velocity profiles for different values of ϕ.

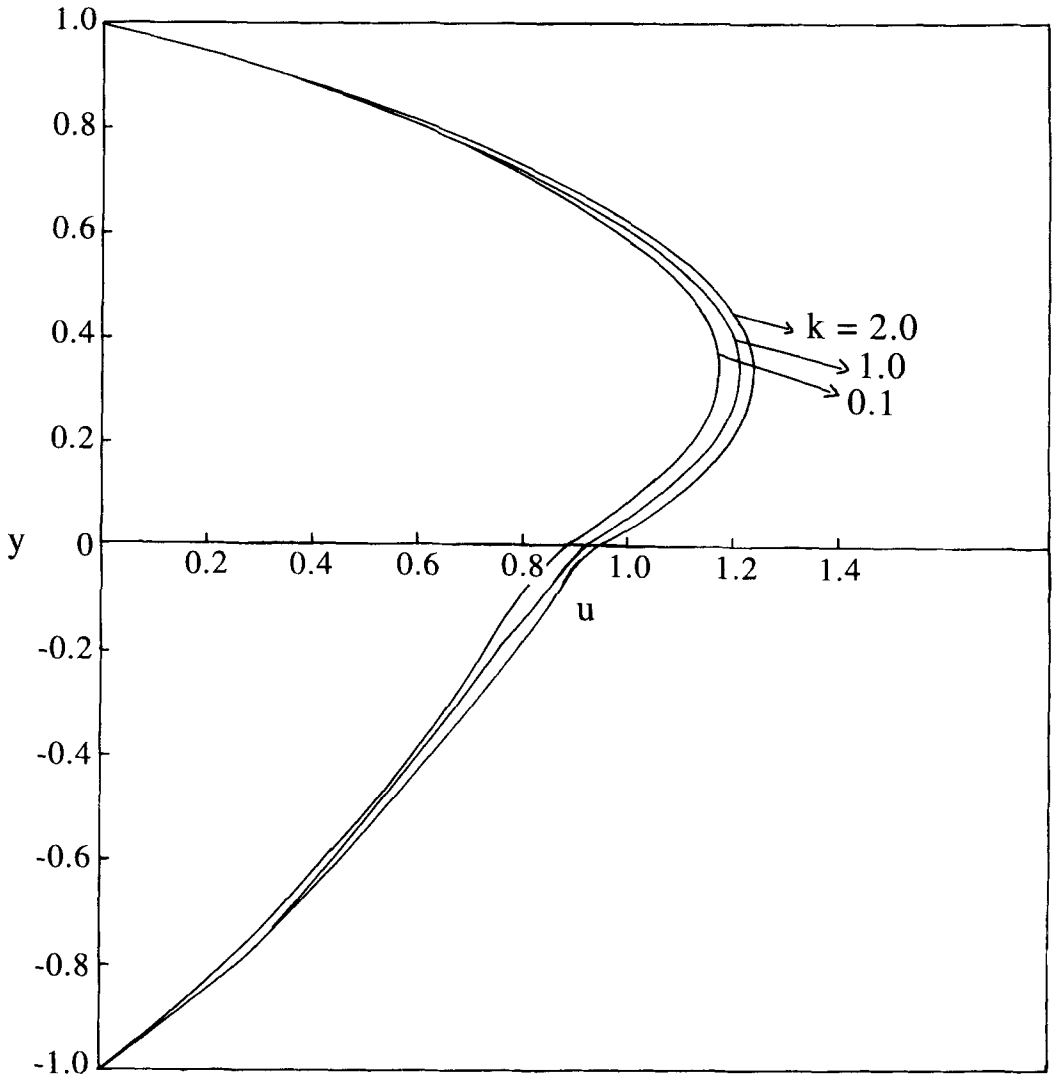

Figure 6. Velocity profiles for different values of k.

$$u_{10}(1) = 0$$

$$u_{10}(0) = u_{20}(0) \qquad [24]$$

$$u_{20}(-1) = 0$$

$$\mathrm{d}u_{10}/\mathrm{d}y = (1/mh)\mathrm{d}u_{20}/\mathrm{d}y \quad \text{at} \quad y = 0.$$

$$\theta_{10}(1) = 1$$

$$\theta_{10}(0) = \theta_{20}(0) \qquad [25]$$

$$\theta_{20}(-1) = 0$$

$$\mathrm{d}\theta_{10}/\mathrm{d}y = (1/kh)\mathrm{d}\theta_{20}/\mathrm{d}y \quad \text{at} \quad y = 0.$$

$$u_{11}(1) = 0$$

$$u_{11}(0) = u_{21}(0) \qquad [26]$$

$$u_{21}(-1) = 0$$

$$du_{11}/dy = (1/mh)du_{21}/dy \quad \text{at} \quad y = 0.$$

$$\theta_{11}(1) = 0$$

$$\theta_{11}(0) = \theta_{21}(0) \qquad [27]$$

$$\theta_{21}(-1) = 0$$

$$d\theta_{11}/dy = (1/kh)d\theta_{21}/dy \quad \text{at} \quad y = 0.$$

Solutions of [16], [17] and [20], [21] using boundary conditions [24] and [25] are:

$$\theta_{10} = (y + kh)/(1 + kh) \qquad [28]$$

$$\theta_{20} = kh(y + 1)/(1 + kh) \qquad [29]$$

$$u_{10} = a_1y^3 + a_2y^2 + c_1y + c_2 \qquad [30]$$

$$u_{20} = d_1 \text{coshM}y + d_2 \text{sinhM}y + f_1 + f_2y \qquad [31]$$

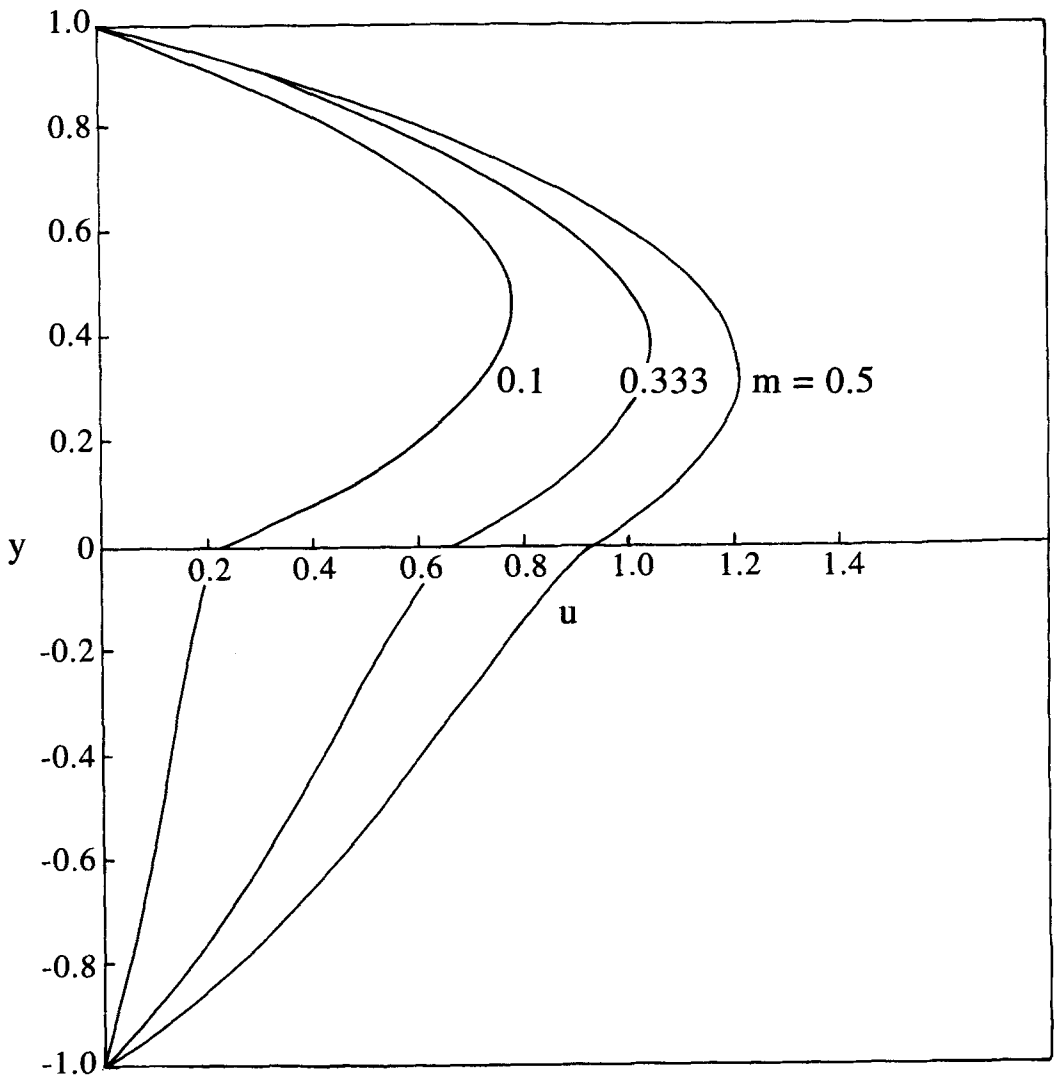

Figure 7. Velocity profiles for different values of m.

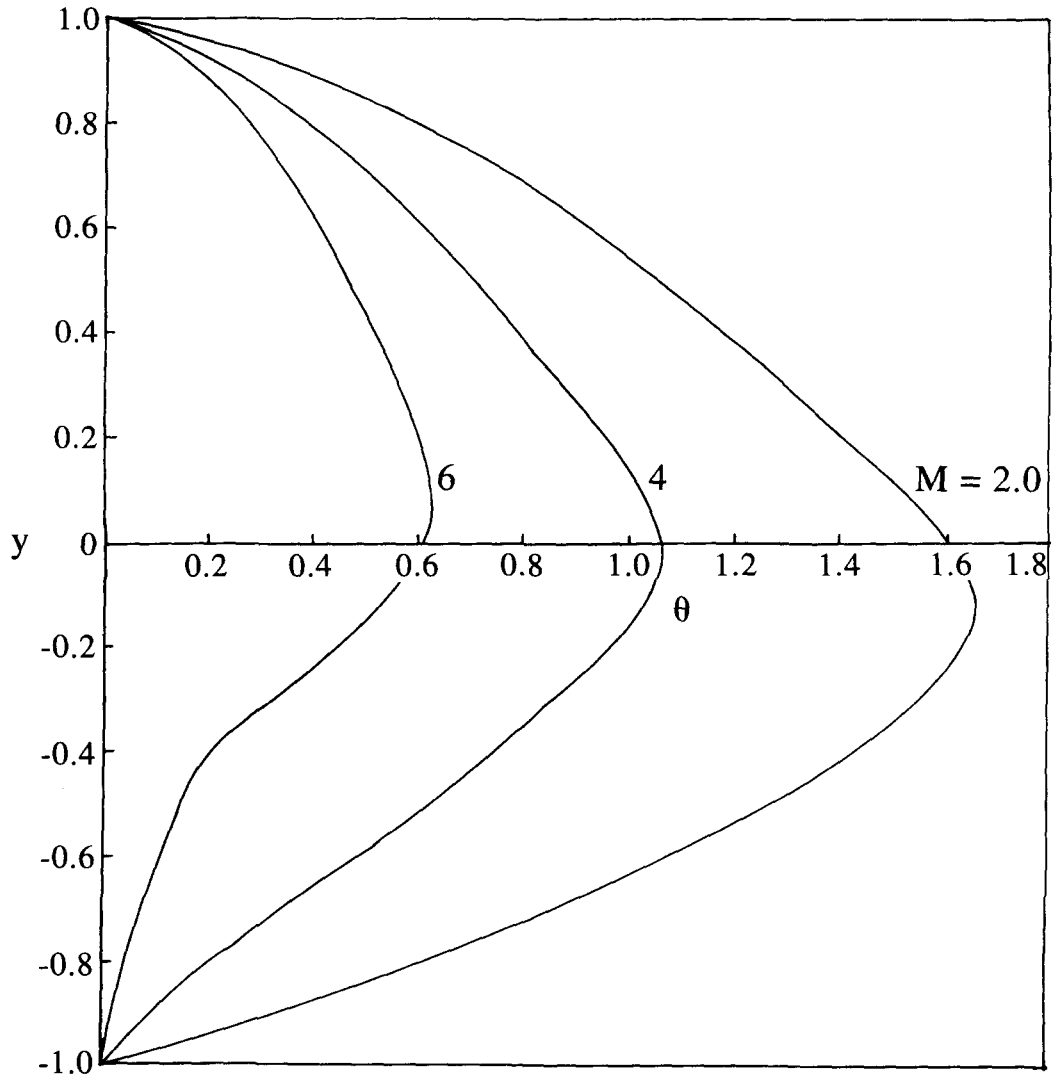

Figure 8. Temperature correction profiles for different values of M.

where

$$G = \frac{\mathrm{Gr}}{\mathrm{Re}} \sin\phi, \quad a_1 = -\left(\frac{G}{6(1+kh)}\right), \quad a_2 = \frac{1}{2}\left(P - \frac{khG}{1+kh}\right),$$

$$f_2 = \frac{kGbmnh^3}{\mathrm{M}^2(1+kh)}, \quad f_1 = -\frac{mh^2P}{\mathrm{M}^2} + f_2,$$

$$d_2 = \frac{mh}{\mathrm{M}\cosh\mathrm{M} + mh\sinh\mathrm{M}}\left\{-\left(a_2 + a_1 + \frac{f_2}{mh} + f_1\right)\cosh\mathrm{M} + f_1 - f_2\right\},$$

$$d_1 = \left(d_2\sinh\mathrm{M} - f_1 + f_2\right)/\cosh\mathrm{M}, \quad c_1 = \left(d_2\mathrm{M} + f_2\right)/mh, \quad c_2 = d_1 + f_1.$$

Solutions of [18], [19] and [22], [23] using boundary conditions [26] and [27] are:

$$\theta_{11} = g_1y^6 + g_2y^5 + g_3y^4 + g_4y^3 + g_5y^2 + e_1y + e_2 \qquad [32]$$

$$\theta_{21} = g_6 \cosh 2My + g_7 \sinh 2My + g_8 y \cosh My + g_9 y \sinh My + g_{10} \cosh My + g_{11} \sinh My + g_{12} y^4 + g_{13} y^3 + g_{14} y^2 + e_1 y + e_2 \quad [33]$$

$$u_{11} = r_1 y^8 + r_2 y^7 + r_3 y^6 + r_4 y^5 + r_5 y^4 + r_6 y^3 + r_7 y^2 + j_1 y + j_2 \quad [34]$$

$$u_{21} = j_3 \cosh My + j_4 \sinh My + p_1 \cosh 2My + p_2 \sinh 2My + p_3 y^2 \cosh My + p_4 y^2 \sinh My + p_5 y \cosh My + p_6 y \sinh My + p_7 \cosh My + p_8 \sinh My + p_9 y^4 + p_{10} y^3 + p_{11} y^2 + p_{12} y + p_{13} \quad [35]$$

where

$$g_1 = -\frac{3a_1^2}{10}, \quad g_2 = -\frac{3a_1 a_2}{5}, \quad g_3 = -\frac{2a_2^2 + 3c_1 a_1}{6},$$

$$g_4 = -\frac{2a_2 c_1}{3}, \quad g_5 = -\frac{c_1^2}{2}, \quad t_1 = -\frac{k\mathrm{M}^2}{m}(d_1^2 + d_2^2),$$

$$t_2 = -\frac{2kd_1 d_2 \mathrm{M}^2}{m}, \quad t_3 = -\frac{2kd_1 f_2 \mathrm{M}^2}{m}, \quad t_4 = -\frac{2kd_2 f_2 \mathrm{M}^2}{m},$$

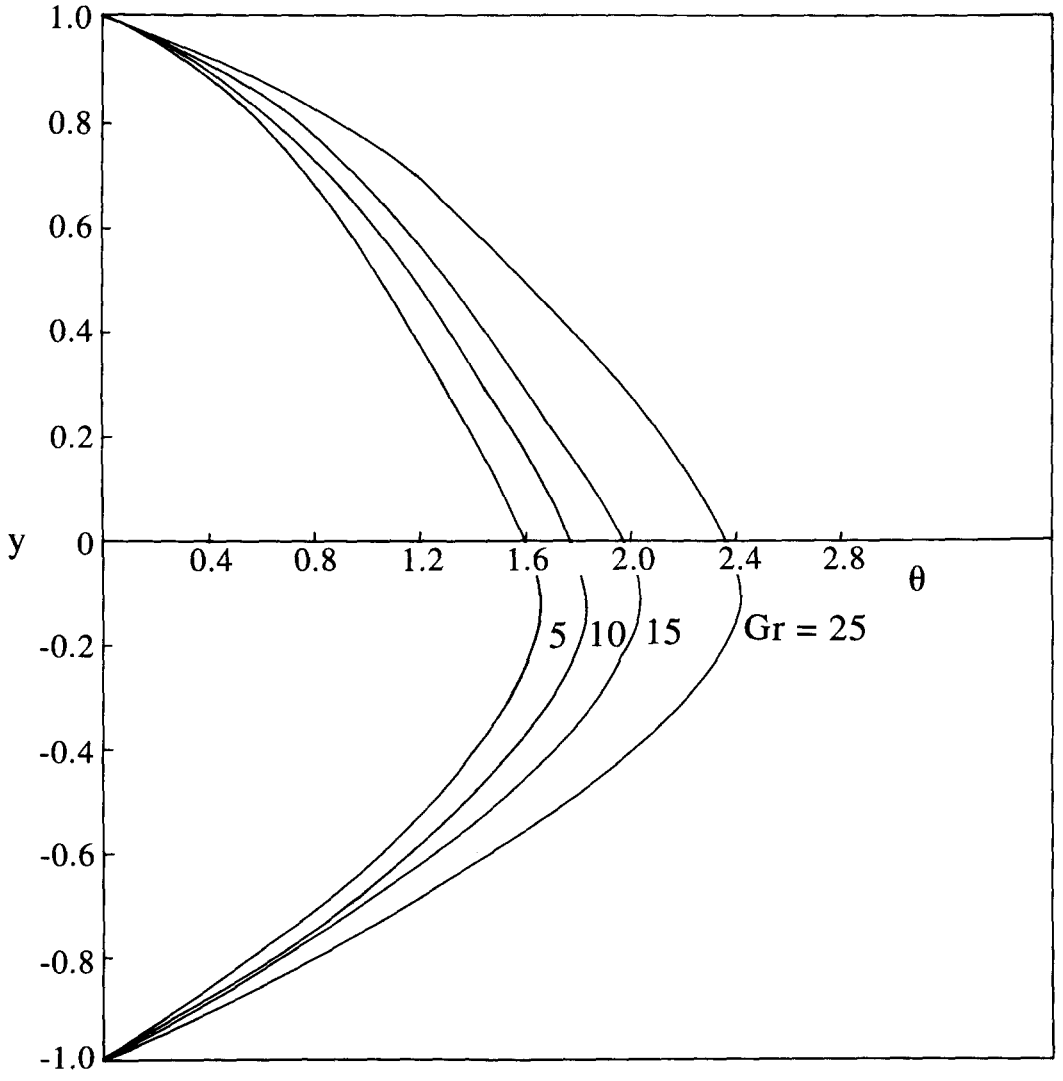

Figure 9. Temperature correction profiles for different values of Gr.

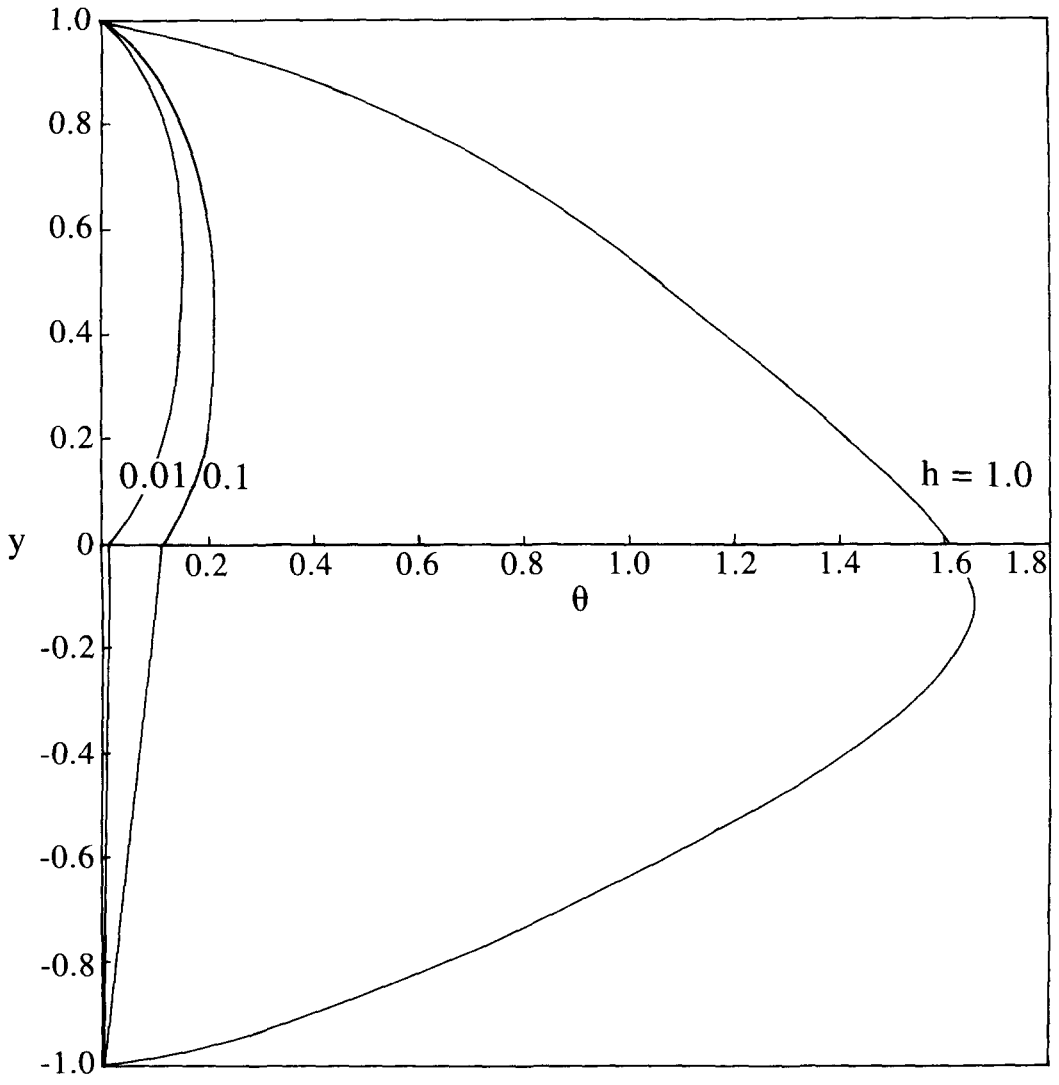

Figure 10. Temperature correction profiles for different values of h.

$$t_5 = -\frac{2k\mathrm{M}}{m}(d_1 f_1 \mathrm{M} + d_2 f'2), \quad t_6 = -\frac{2k\mathrm{M}^2}{m}(d_1 f_2 + d_2 f_1),$$

$$t_7 = -\frac{k\mathrm{M}^2 f_2^2}{m}, \quad t_8 = -\frac{2k f_1 f_2 \mathrm{M}^2}{m}, \quad t_9 = -\frac{k\mathrm{M}^2 f_1^2}{m},$$

$$g_6 = \frac{t_1}{4\mathrm{M}^2}, \quad g_7 = \frac{t_2}{4\mathrm{M}^2}, \quad g_8 = \frac{t_3}{\mathrm{M}^2},$$

$$g_9 = \frac{t_4}{\mathrm{M}^2}, \quad g_{10} = \frac{t_5}{\mathrm{M}^2} - \frac{2t_4}{\mathrm{M}^3}, \quad g_{11} = \frac{t_6}{\mathrm{M}^2} - \frac{2t_3}{\mathrm{M}^3},$$

$$g_{12} = \frac{t_7}{12}, \quad g_{13} = \frac{t_8}{6}, \quad g_{14} = \frac{t_9}{2},$$

$$e_1 = \frac{1}{1+kh}(g_6 \cosh 2\mathrm{M} - g_7 \sinh 2\mathrm{M} + (g_{10} - g_8)\cosh \mathrm{M}$$

$$+ (g_9 - g_{11})\sinh \mathrm{M} + g_{12} - g_{13} + g_{14} + 2\mathrm{M}g_7 + g_8 + \mathrm{M}g_{11} - (g_6 + g_{10} + g_1 + g_2 + g_3 + g_4 + g_5)),$$

$$e_2 = -(g_1 + g_2 + g_3 + g_4 + g_5 + e_1),$$

$$e_3 = khe_1 - 2Mg_7 - g_8 - Mg_{11}, \quad e_4 = e_2 - g_6 - g_{10},$$

$$r_1 = -\frac{Gg_1}{56}, \quad r_2 = -\frac{Gg_2}{42}, \quad r_3 = -\frac{Gg_3}{30},$$

$$r_4 = -\frac{Gg_4}{20}, \quad r_5 = -\frac{Gg_5}{12}, \quad r_6 = -\frac{Ge_1}{6},$$

$$r_7 = -\frac{Ge_2}{2}, \quad \bar{p} = bmnGh^2,$$

$$p_1 = -\frac{\bar{p}g_6}{3M^2}, \quad p_2 = -\frac{\bar{p}g_7}{3M^2}, \quad p_3 = -\frac{\bar{p}g_9}{4M},$$

$$p_4 = -\frac{\bar{p}g_8}{4M}, \quad p_5 = -\bar{p}\left(\frac{g_{11}}{2M} - \frac{g_8}{4M^2}\right), \quad p_6 = -\bar{p}\left(\frac{g_{10}}{2M} - \frac{g_9}{4M^2}\right),$$

$$p_7 = -\frac{\bar{p}g_9}{8M^3}, \quad p_8 = -\frac{\bar{p}g_8}{8M^3}, \quad p_9 = \frac{\bar{p}g_{12}}{M^2}, \quad p_{10} = \frac{\bar{p}g_{13}}{M^2},$$

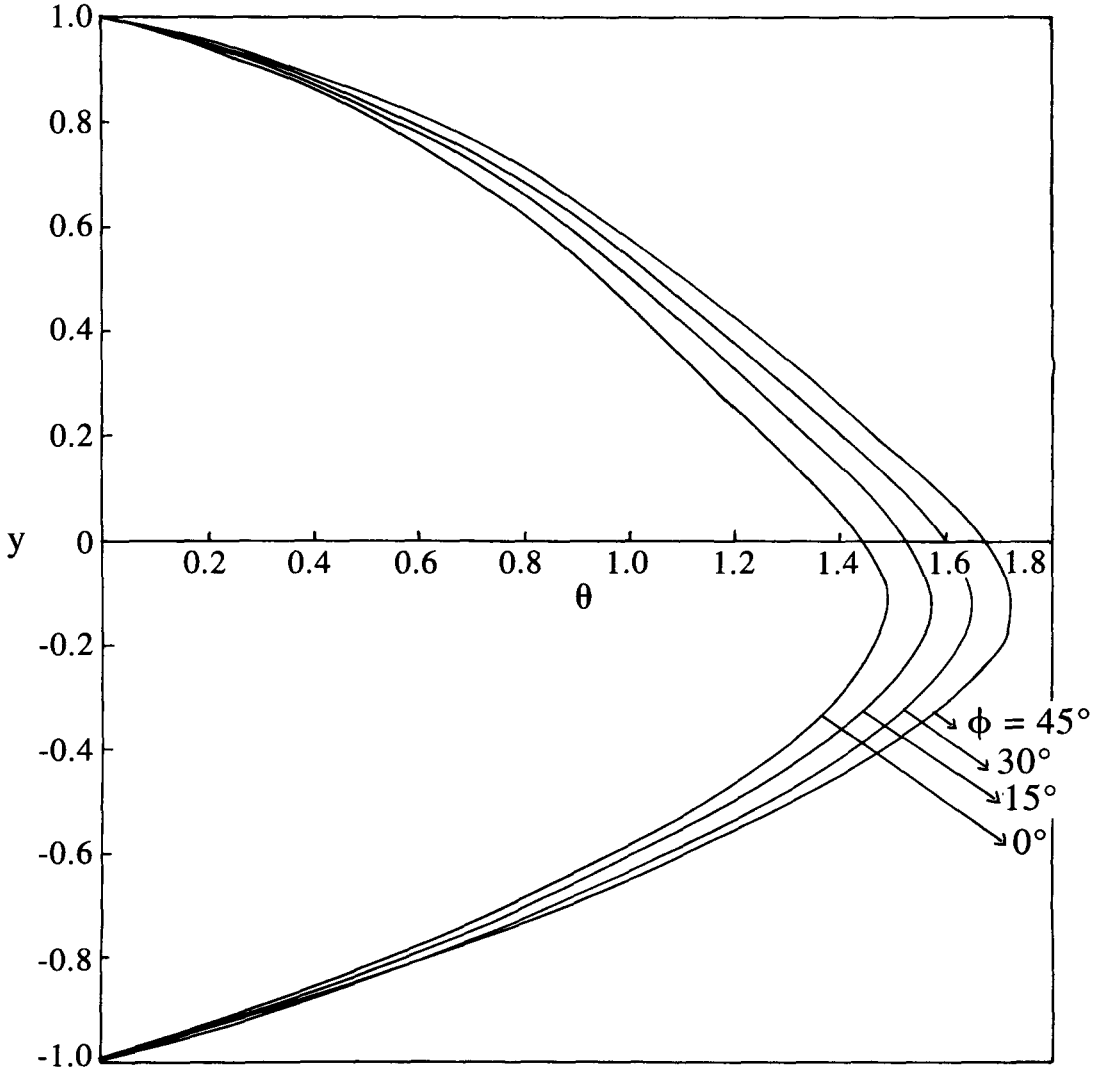

Figure 11. Temperature correction profiles for different values of ϕ.

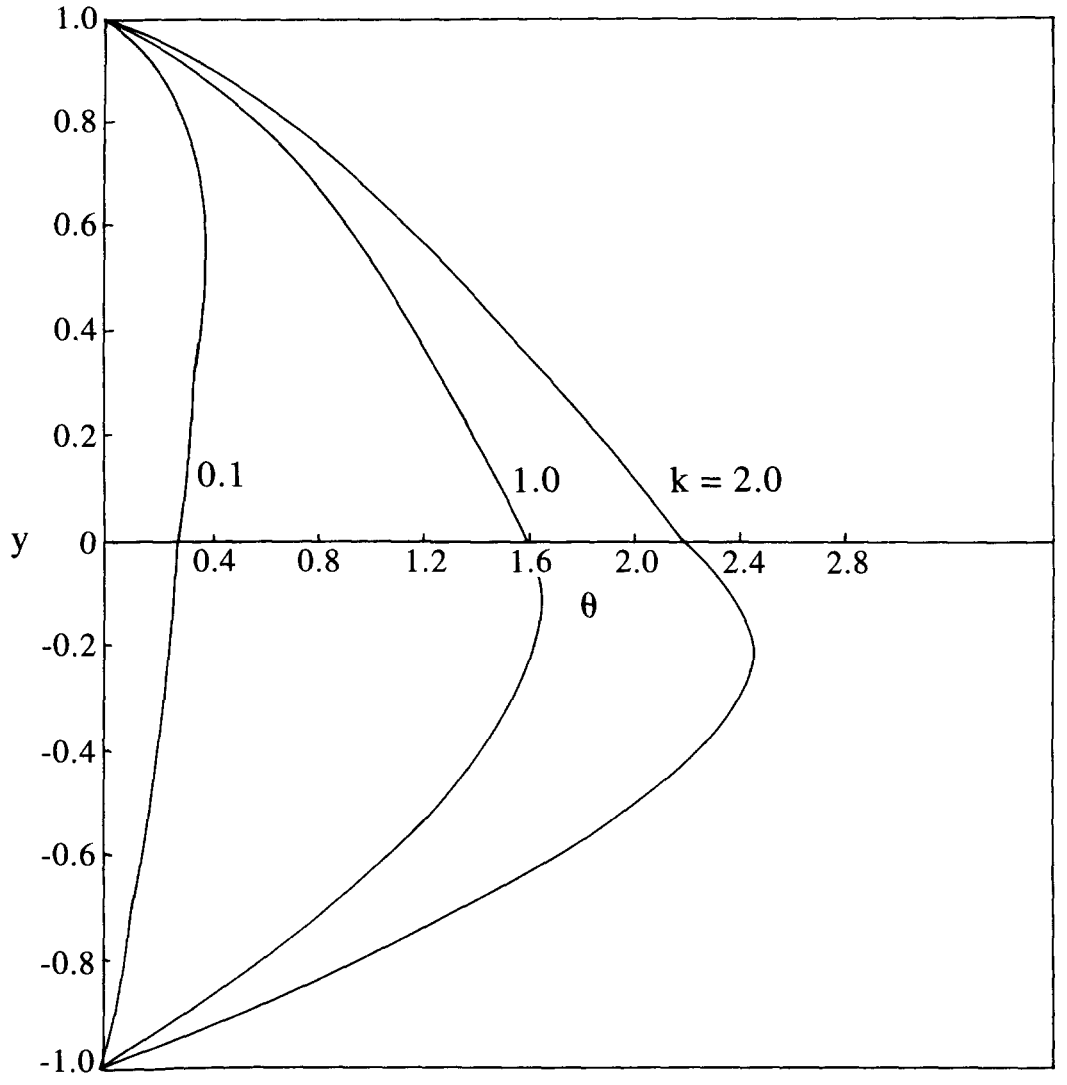

Figure 12. Temperature correction profiles for different values of K.

$$p_{11} = \frac{\tilde{p}}{M^2}\left(g_{14} + \frac{12g_{12}}{M^2}\right), \quad p_{12} = \frac{\tilde{p}}{M^2}\left(e_3 + \frac{6g_{13}}{M^2}\right),$$

$$p_{13} = \frac{\tilde{p}}{M^2}\left(e_4 + \frac{2g_{14}}{M^2} + \frac{24g_{12}}{M^4}\right),$$

$$j_1 = \frac{M}{mh\,\sinh M + M\cosh M}(p_1\cosh 2M - p_2\sinh 2M$$

$$+ \cosh M[-p_1 - p_{13} + p_3 - p_2 - (r_1 + r_2 + r_3 + r_4 + r_5 + r_6 + r_7)]$$

$$+ \sinh M\left[2p_2 + p_6 - p_4 + \frac{p_{12} + p_5}{M}\right] + p_9 - p_{10} + p_{11} - p_{12} + p_{13}),$$

$$j_2 = -j_1 - (r_1 + r_2 + r_3 + r_4 + r_5 + r_6 + r_7),$$

$$j_3 = j_2 - p_1 - p_7 - p_{13}, \quad j_4 = \frac{1}{M}\left[j_1 mh - 2Mp_2 - p_5 - Mp_8 - p_{12}\right].$$

Equations [28]–[35] are evaluated numerically and the results are discussed in section 4. Since the problem involves too many nondimensional parameters, for the sake of conciseness, we fixed some of the parameters namely $P = 5$, $b = 1.0$, $n = 1.5$ and $\mathrm{Re} = 5.0$ for all the numerical computations and analysed the effect of other important parameters on flow and heat transfer. In each illustration, all parameters except the varying one are chosen from the set: (M, Gr, h, m, k, ϕ) = (2.0, 5.0, 1.0, 0.5, 1.0, 30°). The velocity distributions are computed up to first order, i.e. $u = u_i = u_{i0} + \epsilon u_{i1}$ $(i = 1, 2)$ and these velocity distributions are shown in figures. In case of the temperature distributions, only first order temperature is shown in figures, since the zeroth order temperature profiles are linear ([28], [29]).

4. CONCLUSIONS

MHD two-phase flow and heat transfer in an inclined channel is investigated analytically. The resulting governing equations are coupled and nonlinear. These nonlinear equations are solved

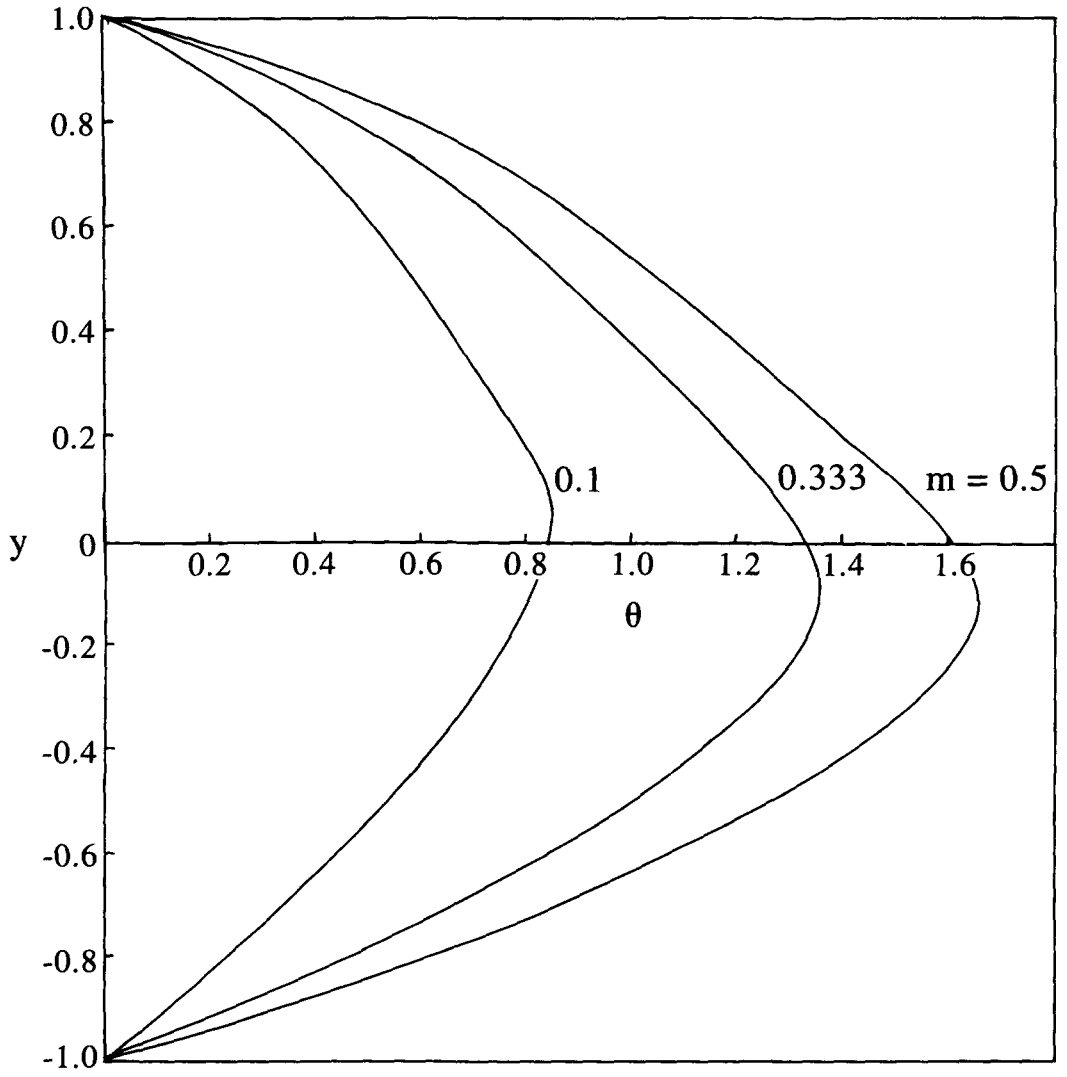

Figure 13. Temperature correction profiles for different values of m.

using the regular perturbation method with the product of Prandtl number and the Eckert number as the perturbation parameter.

The effect of magnetic field on velocity is shown in figure 2. We observe that the effect of increasing magnetic field strength is to dampen the velocity. This is the classical Hartmann result. Figure 3 shows the effect of Grashof number on the flow. The effect of increasing Grashof number is to increase the velocity field. Physically, an increase in the value of Grashof number indicates an increase of buoyancy forces which support the flow. The effect of the ratio of the heights of the fluids on velocity is shown in figure 4. We observe that the smaller the height of the upper electrically nonconducting phase, compared to the lower phase, the larger the flow field. Figure 5 shows the effect of the angle of inclination on velocity. We find that an increase in the value of the angle increases the velocity. The effect of the ratio of the thermal conductivities on velocity is found to be insignificant (see figure 6). The effect of the ratio of the viscosities on velocity is shown in figure 7. We conclude from this figure that, the smaller the value of the viscosity of the fluid in the lower phase compared to the fluid in the upper phase, the larger the flow field.

The first order temperature correction profiles are shown in figure 8 for different values of the Hartmann number M. We find that the magnetic field reduces the effect of dissipations. Figure 9 shows the effect of the Grashof number on temperature. Its effect is to increase the temperature. The effect of the ratio of heights on temperature field is the same as its effect on velocity (figure 10). That is, the smaller the height of the upper phase compared to the lower phase, the larger the magnitude of the temperature. The effect of the angle of inclination on temperature correction is same as its effect on velocity (see figure 11). The effect of the ratio of the thermal conductivities of the two fluids on temperature is shown in figure 12. We find that the temperature increases with the increase in the value of the ratio k, implying that, the fluid in phase I with thermal conductivity better than that of phase II, adds to the heat transfer. The effect of the ratio of viscosities on temperature is shown in figure 13. We find that its effect on temperature is same as that of its effect on velocity field. The less viscous fluid in the lower phase adds to heat transfer.

Acknowledgement—The authors thank the referee for his useful suggestions.

REFERENCES

Catton, I. (1978) Natural convection in enclosures. *6th National Heat Transfer Conf.*, Toronto, Vol. 6, pp. 13–43.

Lohrasbi, J. and Sahai, V. (1988) Magnetohydrodynamic heat transfer in two-phase flow between parallel plates. *Appli. Sci. Res.* **45,** 53–66.

Malashetty, M. S. and Leela, V. (1991) Magnetohydrodynamic heat transfer in two fluid flow. *Proc. National Heat Transfer Conf. AIChE & ASME, HTD*, p. 159.

Malashetty, M. S. and Leela, V. (1992) Magnetohydrodynamic heat transfer in two phase flow. *Int. J. Engng Sci.* **30,** 371–377.

Packham, B. A. and Shail, R. (1971) Stratified laminar flow of two immiscible fluids. *Proc. Camb. Phil. Soc.* **69,** 443–448.

Postlethwaite, A. W. and Sluyter, M. M. (1978) MHD heat transfer problems—an overview. *ASME, Mech. Eng.* **100,** 32–39.

Raithby, G. D and Hollands, K. G. T. (1984) Natural convection. In *Handbook of Heat Transfer*, eds W. M. Rohsnow, J. P. Hartnett and E. Genic, 2nd edn. McGraw-Hill, New York.

Shail, R. (1973) On laminar two-phase flow in magnetohydrodynamics. *Int. J. Engng Sci.* **11,** 1103–1108.

Thome, R. J. (1964) Effect of transverse magnetic field on vertical two-phase flow through a rectangular channel. Argonne National Laboratory Report, ANL 6854.